Title

Corrigendum: Spring land temperature anomalies in northwestern US and the summer drought over Southern Plains and adjacent areas (2016 Environ. Res. Lett. 11 044018)

Journal

Environmental Research Letters, 11(5)

ISSN

1748-9318

Authors

Xue, Yongkang
Oaida, Catalina M
Diallo, Ismaila
et al.

Publication Date

2016-05-01

DOI

10.1088/1748-9326/11/5/059502

Peer reviewed

Spring land temperature anomalies in northwestern US and the summer drought over Southern Plains and adjacent areas

2016 Environ. Res. Lett. 11 044018

(http://iopscience.iop.org/1748-9326/11/4/044018)

Environmental Research Letters

CrossMark

OPEN ACCESS

RECEIVED
9 November 2015

REVISED
25 February 2016

ACCEPTED FOR PUBLICATION
24 March 2016

PUBLISHED
13 April 2016

LETTER

Spring land temperature anomalies in northwestern US and the summer drought over Southern Plains and adjacent areas

Yongkang Xue[1,2], Catalina M Oaida[2], Ismaila Diallo[1], J David Neelin[2], Suosuo Li[1,3], Fernando De Sales[1,4], Yu Gu[2], David A Robinson[5], Ratko Vasic[6] and Lan Yi[7]

[1] Department of Geography, University of California, Los Angeles, CA 90095, USA
[2] Department of Atmospheric & Oceanic Sciences, University of California, Los Angeles, CA 90095, USA
[3] Cold and Arid Regions Environmental and Engineering Research Institute, Chinese Academy of Sciences, Lanzhou, 730000, People's Republic of China
[4] San Diego State University, San Diego, CA 92182
[5] Department of Geography, Rutgers University, Piscataway, NJ 08854, USA
[6] National Center for Environmental Prediction, College Park, MD 20740, USA
[7] Chinese Academy of Meteorological sciences, Beijing, 10081, People's Republic of China

E-mail: yxue@geog.ucla.edu

Keywords: land temperature, US drought and heat, regional climate model, southern great plains, sea surface temperature

Supplementary material for this article is available online

Abstract

Recurrent drought and associated heatwave episodes are important features of the US climate. Many studies have examined the connection between ocean surface temperature changes and conterminous US droughts. However, remote effects of large-scale land surface temperature variability, over shorter but still considerable distances, on US regional droughts have been largely ignored. The present study combines two types of evidence to address these effects: climate observations and model simulations. Our analysis of observational data shows that springtime land temperature in northwest US is significantly correlated with summer rainfall and surface temperature changes in the US Southern Plains and its adjacent areas. Our model simulations of the 2011 Southern Plains drought using a general circulation model and a regional climate model confirm the observed relationship between land temperature anomaly and drought, and suggest that the long-distance effect of land temperature changes in the northwest US on Southern Plains droughts is probably as large as the more familiar effects of ocean surface temperatures and atmospheric internal variability. We conclude that the cool 2011 springtime climate conditions in the northwest US increased the probability of summer drought and abnormal heat in the Southern Plains. The present study suggests a strong potential for more skillful intra-seasonal predictions of US Southern Plains droughts when such facts as ones presented here are considered.

1. Introduction

Recurrent drought and associated heatwave episodes are important features of the conterminous United States climate [1]. Many analyses of US drought data show that the Great Plains is one of the most drought-prone regions across the nation [2–4]. US droughts have been attributed to various mechanisms, including natural variability of the Great Plains climate (i.e. the great droughts there seem to occur once or twice a century [5, 6]), the presence of an atmospheric circulation pattern at the beginning of a period leading to anomalies and/or preferred atmospheric conditions for maintenance of the drought [7, 8], effects of soil moisture and land conditions [8–12], and teleconnection with sea surface temperature (SST) anomalies. Of these, SST anomalies have been studied the most as a factor responsible for drought. The key finding is that the El Niño–Southern Oscillation and the Pacific decadal oscillation (PDO) in their cold phases and the Atlantic Multidecadal Oscillation in its warm phase tend to cause droughts over the US, with

the Pacific Ocean playing the dominant role [2, 13–17]. The studies showed statistically significant correlations above ~0.3 at the 0.05 level between Pacific SST and droughts in the Great Plains and the adjacent southwest [18–20]. Modeling studies confirm observational findings in support of the important role SSTs play in US drought. However, SST fluctuations alone only partially account for drought severity and recurrence [21]. Here we explore a new approach to understand the 2011 Texas drought by identifying remote land surface temperature (LST) and land-atmospheric interactions as notable contributors.

2. Methods

The present study combines both climate observations and model simulations to investigate the remote effects of spring LST and subsurface soil temperature (SUBT) anomalies in the northwest US (NWUS, 117 °W–125 °W and 33 °N–49.8 °N (land only))[8] as contributing factors to drought in the US Southern Great Plains and its adjacent areas, including some areas to the east of the Southern Great Plains (SGP, 88 °W–103 °W and 29 °N–38 °N)[9]. Ground measurements from the Climate Prediction Center's global gauge-based analysis of precipitation and surface temperature (GTS) [22] and surface temperature station data from the Climate Anomaly Monitoring System (CAMS) [23], as well as the Rutgers University Global Snow Lab snow cover extent data (all of which cover the period from 1980 through 2011) were used to study the relationship between LST in the NWUS and precipitation in the SGP, as well as the contribution of snow cover in western US coastal area to this relationship. A recent study found that since 1980, the precipitation decrease in Central US has intensified [17].

Furthermore, to test these observed relationships and the hypothesis that abnormally cold NWUS spring conditions may have contributed to the 2011 June–July SGP record drought and heat anomalies, and to compare LST and SUBT effects with SST forcing, the WRF-NMM regional climate model (RCM) with 50 km horizontal resolution and the NCEP Global Forecast System (GFS) with T62 horizontal resolution were employed for numerical sensitivity studies. Both were coupled with the Simplified Simple Biosphere model (SSiB) [24], which is a biophysically based model that simulates land-atmosphere interactions by calculating the surface energy budget and surface water balance for three soil layers and one vegetation layer. A force–restore method [25] was used to calculate the heat transfer between the surface and subsurface soil layers.

[8] See red box in figure 2(a) for reference.

[9] See box in figure 2(b) for reference.

3. Results

3.1. Observational evidence

Although the SST remote effects on the drought have been extensively investigated, paradoxically, less attention has been devoted to the effects of large-scale LST, over shorter but still considerable distances, on US regional droughts, despite the fact that the areas with LST anomalies are geographically closer to the drought area than the areas with SST anomalies.

While there have been studies that suggest an inverse relationship between spring snow mass (which is closely linked to LST) in the western US and subsequent summer precipitation over the US southwest associated with the North American monsoon system [26, 27], this snow–monsoon relationship has been unstable over time and space, showing a peculiar on-and-off characteristic in the last century [28], and its effect on monsoon through soil moisture has been challenged in another study [29]. Using the GTS and CAMS surface temperature station data from 1980 through 2011, we examine the observed LST–precipitation relationship and find that conditions with cold spring LST in the NWUS have a high probability of being associated with drier and warmer summer conditions in the SGP as displayed in figures 1(a) and (c), which show scatter plots of NWUS May LST compared with June precipitation and with surface temperature over the SGP for 1980–2011, respectively. For comparison, the scatter plots of May SST in North East Pacific (NEP) (124 °W–135 °W and 30 °N–50 °N)[10] versus June precipitation and temperature in the SGP are also shown in figures 1(b) and (d), respectively. The domain selections for LST and SST are based on figures 2 and S1, which show maximum anomalies of LST over the NWUS and SST over the NEP, respectively, to be discussed later. The generally positive correlations with precipitation for these 32 years are apparent for both LST and SST, with correlation coefficients of 0.33 and 0.35, respectively, and statistical significance at $\alpha < 0.1$ for the two-sided T-test, which is also used for other statistical tests in this paper. The SST-precipitation correlations are consistent with previously published correlations between the Pacific SST and precipitation in the Great Plains [18–20], which were based on different data sets.

If we select the years with large LST anomalies out of the 32-years record spanning 1980 to 2011, higher correlations amongst NWUS spring temperatures and summer time SGP rainfall and temperature are found. For instance, there were 19 years, 10 cold (1980, 1988, 1990, 1991, 1996, 1998, 1999, 2002, 2010, 2011) and 9 warm (1987, 1992, 1993, 1994, 1997, 2001, 2006, 2007, 2009) (see figure 1(a)), when absolute LST anomalies over the NWUS were larger than 0.6 °C (about half of one standard deviation). Among the 10 cold years (blue diamonds plus red triangle in figure 1(a)), seven

[10] See black box in figure 2(a) and figure S1 for reference.

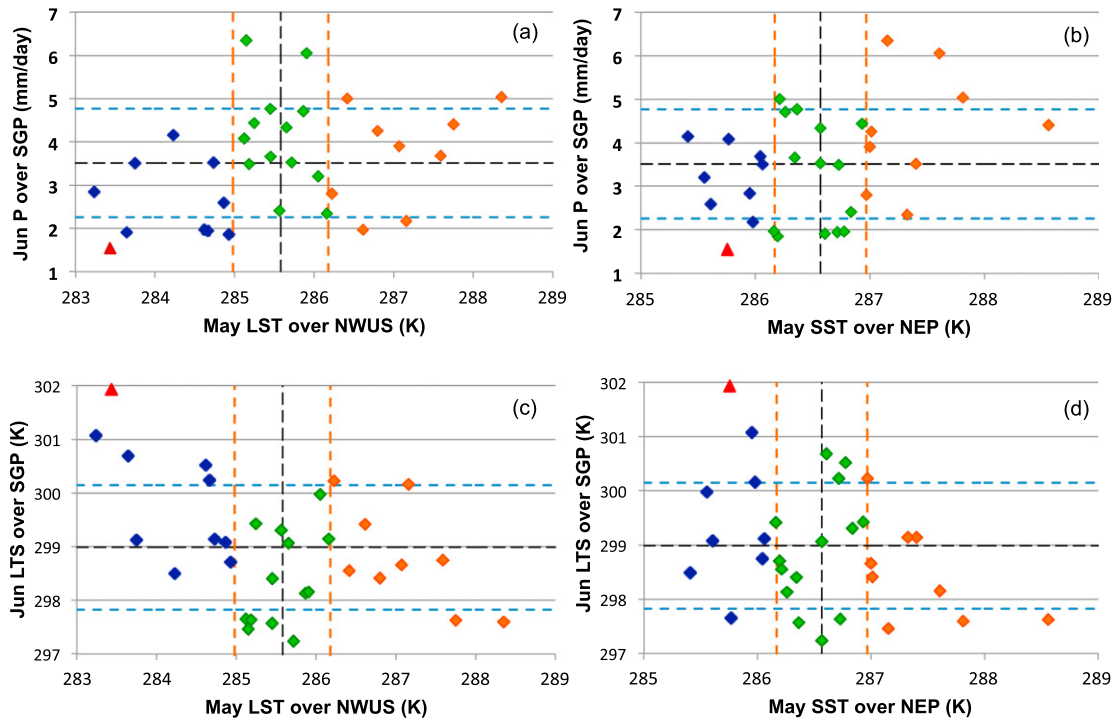

Figure 1. May temperature and June precipitation scatter plots. Left panels: surface temperature; right panels: SST. Study regions are 124–135 °W/30–50 °N for SST (K), 117–125 °W/33–49.8 °N for LST (K), and 88–103 °W/29–38 °N for precipitation (mm/day). Bright red triangles denote year 2011 values. Black dashed lines indicate means; blue dashed lines denote +/−1 standard deviation boundaries for June P (a), (b) and June LST (c), (d) over SGP; orange dashed lines denote +/−0.6 °C for May LST (a), (c) over NWUS and +/−0.4 °C for May SST (b), (d) over NEP. The points are colors coded (blue, green, orange) to represent cool, neutral and warm temperature anomalies.

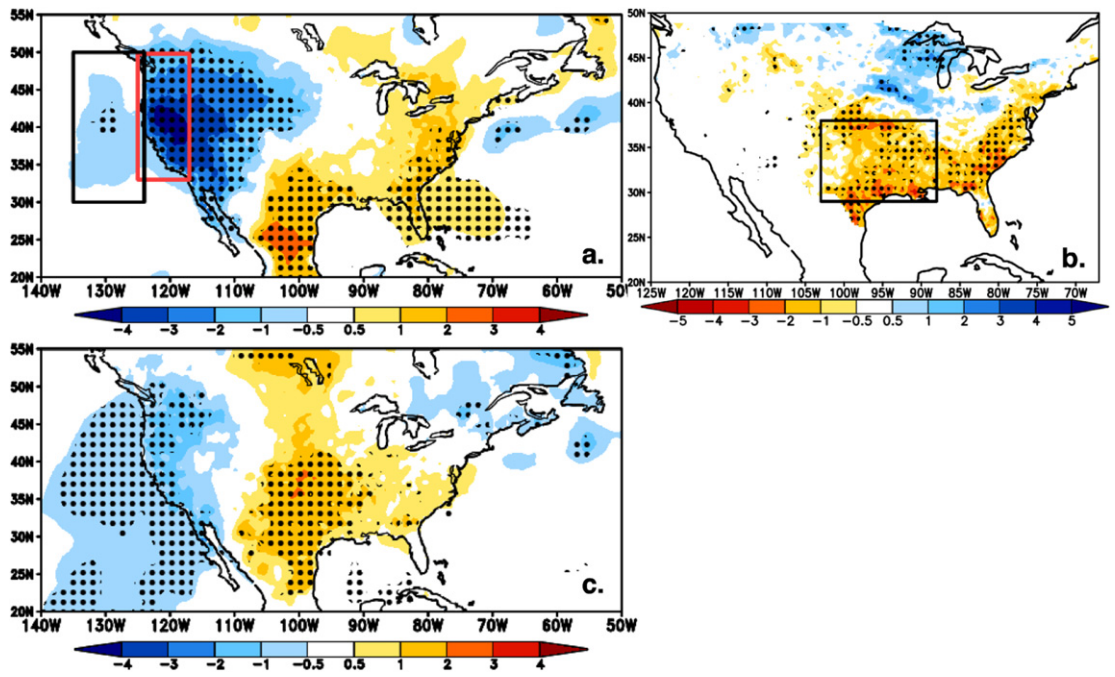

Figure 2. (a) Observed May LST and SST difference (°C) between 9 coldest years and 9 warmest years (based on NWUS LST), (b) observed June precipitation difference (mm day^{-1}) between the same years as in figures 2(a), and (c) observed June LST difference (°C) between the same years as in figure 2(a). The dotted areas denote statistical significance at the $\alpha = 0.01$ level of t-test values.

showed negative June precipitation anomaly over the SGP (with five of those seven years having negative precipitation anomalies exceeding one standard deviation), two were normal, and another had a slight positive anomaly for the area as a whole but a strong negative anomaly near the south Texas coast.

Table 1. Correlation coefficients between LST (K), SST (K), snow extent (%), and precipitation (mm day^{-1}).

	32 years	19 (LST)/18 SST years
May LST in NWUS vs June Precipitation in SGP	0.33*	0.54***
MAY SST in NEP vs June Precipitation in SGP	0.35**	0.50**
May LST in NWUS vs June LST in SGP	−0.46***	−0.68***
May LST in NWUS vs May SST in NEP	0.44***	
May LST in NWUS vs April Snow cover in NWUS	−0.36**	
May LST in NWUS vs May precipitation in NWUS	−0.44***	

See text for areas over which averages were done.
*, **, *** indicate statistics at 0.10, 0.05, and 0.02 significance levels, respectively.

Removing one cold year to have same number of warm and cold years, the correlation between May LST in the NWUS and June precipitation in the SGP for the 18 large anomaly years is 0.53, with statistical significance at $\alpha < 0.05$.

Meanwhile, May LSTs in the NWUS are also negatively correlated with June LSTs in the SGP (figure 1(c)). The correlation coefficients between them for all 32 years and for the 18 large anomaly years are −0.46 and −0.68, respectively, with significance at the 0.01 (table 1). Among the 10 coldest NWUS Mays (blue diamonds plus red triangle in figure 1(c)), five were associated with high positive June temperature anomalies in the SGP exceeding one standard deviation. There were only two other such hot SGP anomaly within the 32-year record not belonging to the ten coldest NWUS Mays (figure 1(c)). The results in figures 1(a) and (c) suggest an association between cold NWUS springs anomalies and a substantially increased probability of summer drought and heat events in the SGP.

To delineate the spatial characteristics of this relationship, figure 2 shows temperature and precipitation differences between the nine coldest and nine warmest years previously discussed. Figure 2(a) shows the May CAMS-observed LST difference. The significant negative temperature anomaly in NWUS is obvious. Cold LST anomalies in NWUS typically emerge in March and are well developed by April and May, ending in June (not shown). Figure 2(b) shows observed negative June rainfall anomalies over the SGP and surrounding areas, from New Mexico to Texas, Oklahoma, Louisiana, and Mississippi, and a slightly positive rainfall band to the north. Warm temperature anomalies in June over the Southern Plains are displayed in figure 2(c). The warm anomaly covers a much larger area compared with the precipitation anomaly, with the heat core further west. Note that all differences in figure 2 are statistically significant at $\alpha < 0.1$ level.

Figure 2(a) also shows SST differences based on Reanalysis data. There is a positive correlation of 0.44 (significant at $\alpha < 0.01$) between May NWUS LST anomalies and May NEP SST anomalies throughout the 32 study years. However, the larger LST and SST anomaly years are not always associated with each other. For example, figure 2(a) shows that although the SST anomaly in NEP is consistent with a NWUS LST anomaly, it is much weaker for those years. There were 18 years (nine very cold and nine very warm years) with absolute NEP SST anomalies larger than 0.4 °C (about half of one standard deviation) (figures 1(b) and (d)) (which again, do not coincide entirely with the 18 years based on May LST discussed earlier). The correlation coefficient between May NEP SST and June SGP precipitation for these 18 years is 0.5, with statistical significance at the 0.05, similar to the LST correlation discussed earlier. For reference, the spatial patterns of the difference between these nine coldest and nine warmest SST years are shown in figure S1; the magnitudes of SST anomaly in these years are much larger than those shown in figure 2(a). The SST spatial anomaly patterns over the Pacific in figure 2(a) and S1 are consistent with the cold phase of the PDO pattern [30]. The warm SSTs over the Gulf of Mexico and nearby Atlantic are also apparent. These ocean patterns are in agreement with the aforementioned previous studies linking SSTs and US drought. Our empirical analysis of correlations between SST/SGP precipitation anomalies is consistent with previous studies [18–20].

The concurrent correlation between May LST in NWUS and SST in NEP, as previously mentioned, has a coefficient of 0.44. We have also computed lag correlation between SST in NEP and LST in NWUS. The correlation coefficients between Feb SST, March SST, and April SST with May LST are only 0.12, 0.21, and 0.28, respectively. The correlation coefficients discussed earlier (and summarized in table 1) suggest that LST and SST may explain a comparable fraction of variance in the SGP precipitation variability. Moreover, previous modeling studies with specified SSTs have also consistently showed that the SST cannot produce the full scope of the droughts [16], and the severity and recurrence of US droughts cannot be explained entirely by the SST fluctuations [21]. These lead us to conjecture that LST anomalies may also significantly contribute to precipitation and heat anomalies in SGP, as it is further tested in this paper.

There are few studies linking the LST anomaly in NWUS to other variables. In addition to the association between LST and SST anomalies as discussed above, investigations based on observational data

from snow course and precipitation sites have established a close relationship between prior winter snowfall/snow cover and spring LST in the NWUS: greater (less) snow water equivalent (SWE) and/or positive (negative) snowfall anomalies [31, 32] are associated with cooler (warmer) surface temperatures. Based on the Rutgers University Global Snow Lab snow cover extent data, we find the correlation between May NWUS LST and April snow cover extent over the area with 118 °W as an eastern boundary, 50 °N as a northern boundary and the coastline as the western and southern boundaries, to be −0.36 at a 0.05 significance level. Meanwhile, the correlation coefficient between NWUS May LST and NWUS May precipitation is −0.44 at 0.02 significance level. A statistically significant correlation between winter precipitation and spring snow cover extent for the 18 years with largest anomalies is also found. Table 1 summarizes the correlations that we discuss above. A better understanding of relationship between spring NWUS LST anomalies and different variables, such as snow, SST, and geothermal heat flow as proposed in the early studies on the subsurface soil temperature anomalies, requires a more comprehensive investigation [31–33], and is of importance in connecting winter/spring precipitation to summer drought from a seasonal forecast perspective.

3.2. Approach of numerical experiments

To further confirm whether the correlations discussed in the last section are more pronounced than expected from random sampling variability, and to understand the causal relationship between these variables, modeling studies are necessary. An exploratory modeling study using the Eta regional climate model (RCM) and the NCEP general circulation model, which studied the effect of warm SUBT over the western US on southern US June wet condition in 1992, suggested that imposed initial warm spring LST and SUBT anomalies in the western US could persist and have an impact on North American June circulation and precipitation [34]. The anomalous perturbation induced by surface heating due to a warm spring western LST and SUBT anomaly propagated eastward through atmospheric Rossby waves within the mean westerly flow. In addition, the steering flow contributed to the dissipation of this perturbation in the northern US and its enhancement in the southern US. These processes led to a positive 1992 June precipitation anomaly in the southern US.

The observational evidence discussed in the last section and our previous modeling results [34] compelled us to evaluate whether this relationship existed during 2011 when severe SGP drought and heat occurred. The 2011 SGP drought intensified rapidly in late spring, and in the summer of 2011 Texas and parts of several surrounding states suffered one of the worst droughts on record in this region [3, 35, 36]. Overall, Texas had its driest year on record (October 2010 to September 2011) at 54% of normal rainfall, and the driest summer on record, with just 62 mm of precipitation. Several climate divisions in Texas and nearby states had record low Palmer Hydrological Drought Index values within the 117-year database [37]. Meanwhile, the 2011 summer positive temperature anomaly of 2.98 °C above the 1981–2010 mean across Texas was larger than the previous record dating back to 1895 [3, 38]. The causes of this great drought are still largely unknown. It has been suggested that summer rainfall deficit over Texas was related to increased convective inhibition due to local soil moisture feedback [11]. Another study links the heat in 2011 to greenhouse gas emissions but does not link to the precipitation deficit [39]. The 2011 extreme SGP drought and heat are highlighted in figure 1. Spring 2011 had high NWUS snowfall [40] and record low LST (−2.16 °C, figure 1(a)). The discussion above suggests such an extreme spring situation could contribute substantially to an increased probability for severe drought in the Southern Plains.

In this study, the NCEP GFS [41] and WRF-NMM RCM [42] are employed. The GFS and WRF have the same SST conditions and initial atmospheric and land surface conditions, but the SST anomaly in the GFS covered the globe based on observational data. The RCM lateral boundary conditions (LBC) were obtained from the corresponding NCEP GFS cases. For example, the WRF LBC for the April 29, 2011 initial condition was obtained from the corresponding NCEP GFS run that was also integrated starting from April 29, 2011. Due to known deficiencies in the global model simulation, we use WRF to downscale the GFS results, which produces better regional simulations. This issue has been discussed in [34] and will be addressed further in the discussion section. This paper only presents the WRF RCM results.

Three numerical experiments (referred to as Case 2011, Case SUBT, and Case SST) with the NCEP GFS and WRF are carried out to integrate the models for three months with five different initial conditions (April 28, 29, 30, May 1, and 2) through July 31, 2011. The sample means from these five integrations with slightly different initial conditions for each Case are presented in this paper. The 2011 drought and heat anomalies are simulated in Case 2011, which uses the 2011 Reanalysis II [43] atmospheric and land data that have abnormal cold LST and SUBT over the NWUS, as initial conditions, as well as 2011 Reanalysis II sea ice and SST that have abnormal cold NEP SST, as boundary conditions for both GFS and WRF. Figure S2 demonstrates that Case 2011 from the RCM run produces a reasonable 2011 June drought and hot conditions over SGP, albeit with some biases. Spatial correlations over US between observations and simulations are 0.91 and 0.67 for temperature and precipitation, respectively. The simulated June precipitation and LST over SGP were 1.07 mm day^{-1}

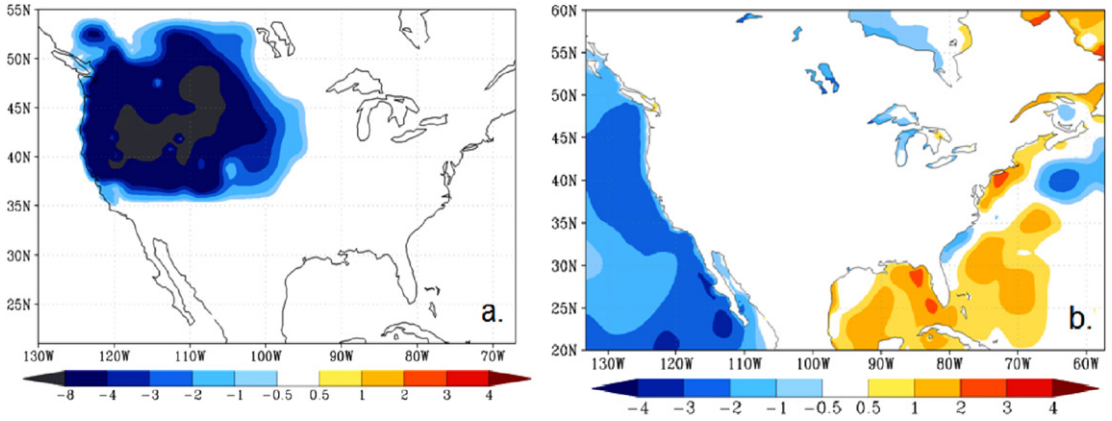

Figure 3. (a) Initial SUBT difference (°C) between Case 2011 and Case SUBT; (b) May SST difference (°C) between Case 2011 and Case SST.

and 304.9 K, respectively, while the observed values were 1.55 mm day^{-1} and 301.9 K, respectively. The 2011 SST, LST, SUBT, and atmospheric internal variability all play a role in the simulation of Case 2011.

The other two experiments are designed to have the same initial atmospheric and surface conditions as Case 2011, but one has warm initial LST and SUBT (Case SUBT) over NWUS, and the other has warm/cold monthly mean SST anomalies over NEP/US Coastal-Atlantic (Case SST), anomalies which were based on the nine warmest NWUS spring LST for Case SUBT and nine warmest NEP spring and summer SST for Case SST, respectively. According to our hypothesis, Case SUBT and Case SST should produce wet summer conditions in SGP due to SUBT and SST effect, respectively. These experiments isolate the potential impact on SGP drought and heat due to these factors.

Based on the high correlation between SUBT and LST [28], observed LST was used as a reference to generate the initial SUBT anomaly in Case SUBT (in absence of large-scale observations for SUBT) as we did in an earlier study [34]. Without an imposed initial SUBT anomaly, any imposed initial LST anomaly would disappear in a couple of days due to thin surface soil layer in the model. The imposed anomalous SUBT was only used as an initial condition in Case SUBT, with SSiB land model updating the SUBT throughout the integrations, helping maintain SUBT anomalies for longer than a couple of days. Figure 3(a) shows the differences in initial SUBT between Case 2011 and Case SUBT. The initial SUBT difference between Case 2011 and Case SUBT in figure 3(a) shows cold SUBT over NWUS. This is consistent with what is shown in figure 2(a) but with larger anomalous magnitudes. The negative anomalous areas are shifted to the north. The initially imposed anomaly can last a little more than a month (from May to early June), similar to the results discussed in [34]. Figure 3(b) shows the spatial patterns of May SST differences between Case 2011 and Case SST in WRF, which are consistent with the difference shown in figure S1 but of larger magnitude. The SST in NEP in May 2011 is cool, as shown in figure 1. The warm SSTs over the Gulf of Mexico and nearby Atlantic are also apparent in figure 3(b).

3.3. Impact of SUBT and SST anomalies

Figures 4(a), 5(a), and 6(a) show the observed differences of June and July LST and June precipitation between 2011 and the means of nine years with the warmest spring LST in the NWUS since 1980 (as discussed in previous section), respectively. They serve as observational benchmarks for comparison to the model-simulated differences between Case 2011 and Case SUBT and between Case 2011 and Case SST, since imposed initial SUBT anomalies in Case SUBT and SST anomaly in Case SST are based on the difference between 2011 and these years. Precipitation and LST differences over the SGP between the various cases presented here are used to assess SGP drought impact due to LST and SST. It is expected that the difference between Case 2011 and Case SUBT would be comparable with the benchmark if SUBT has a substantial impact on drought.

Due to the internal variability in model simulations and in the real world, plus deficiencies in current climate models, the model normally needs to have strong prescribed forcing to produce statistically significant results. In this study, by imposing the larger spring LST perturbations that are comparable to the difference between an extreme cold year (here 2011) and very hot years over NWUS, we aim to obtain a significant June precipitation difference that is comparable to the difference between 2011 and wet years. Use of a relatively large forcing to test a new hypothesis at the preliminarily experimental stage and to understand mechanisms is common [8, 44, 45], while, in fact, our imposed LST anomalies can be compared to those observed.

To facilitate the comparison with the observational data and to emphasize the SUBT effect, Case

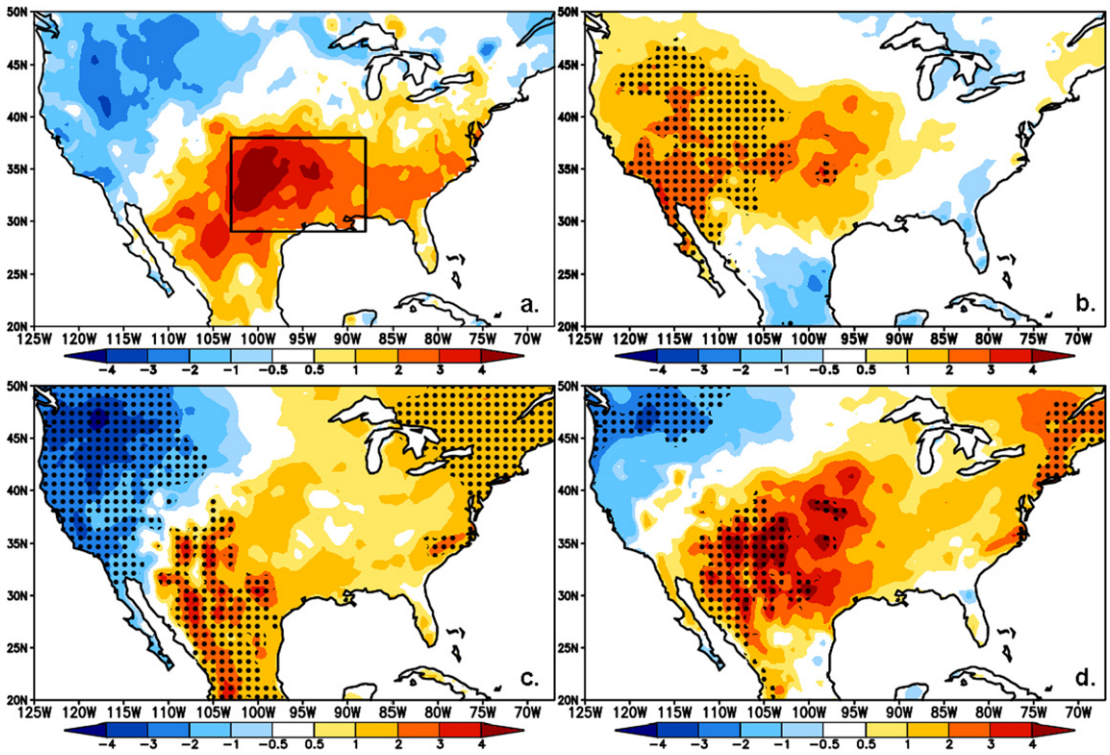

Figure 4. Observed/WRF simulated anomaly/difference of surface temperature (°C) for June. (a) Observed, (b) SUBT effect, (c) SST effect, and (d) SST effect plus SUBT effect. The dotted areas denote statistical significance at the $\alpha = 0.01$ level of t-test values.

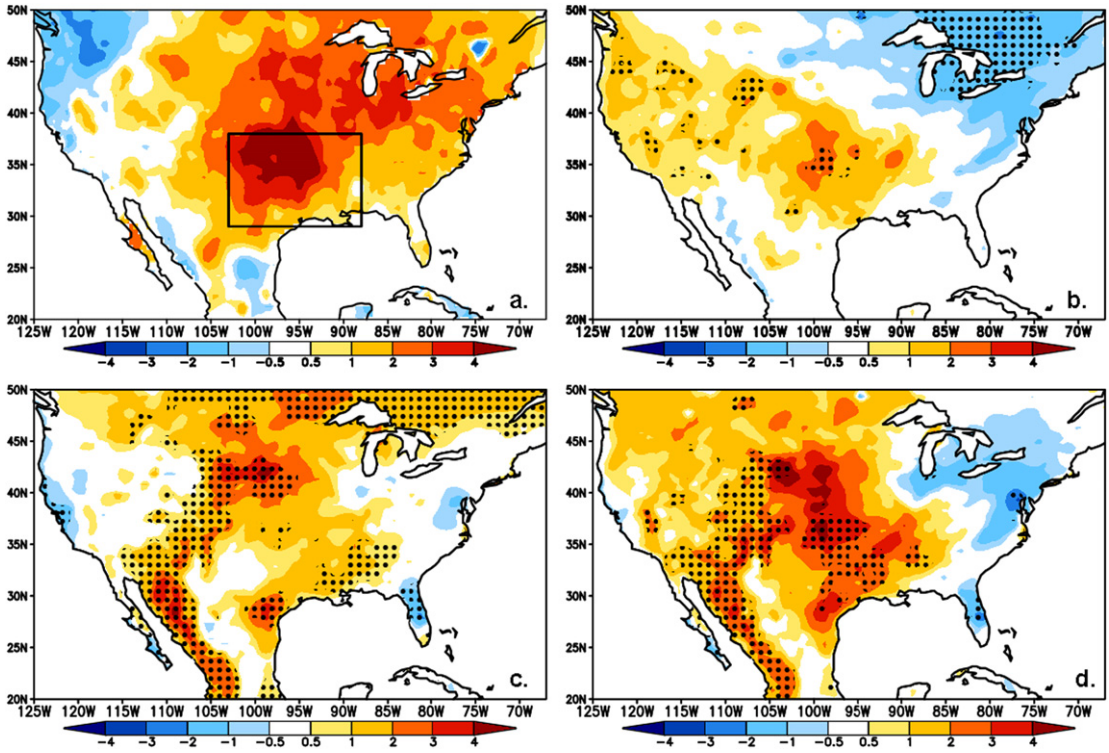

Figure 5. Observed/WRF simulated anomaly/difference of surface temperature (°C) for July. (a) Observed, (b) SUBT effect, (c) SST effect, and (d) SST effect plus SUBT effect. The dotted areas denote statistical significance at the $\alpha = 0.01$ level of t-test values.

SUBT and the sum of Case SUBT + Case SST (referred to as Case SUBTSST) are emphasized. Case SUBTSST does not include the interactions between SST and SUBT, which are assumed to be secondary effects in this study; further tests would be needed to quantify this effect. The difference between Case 2011

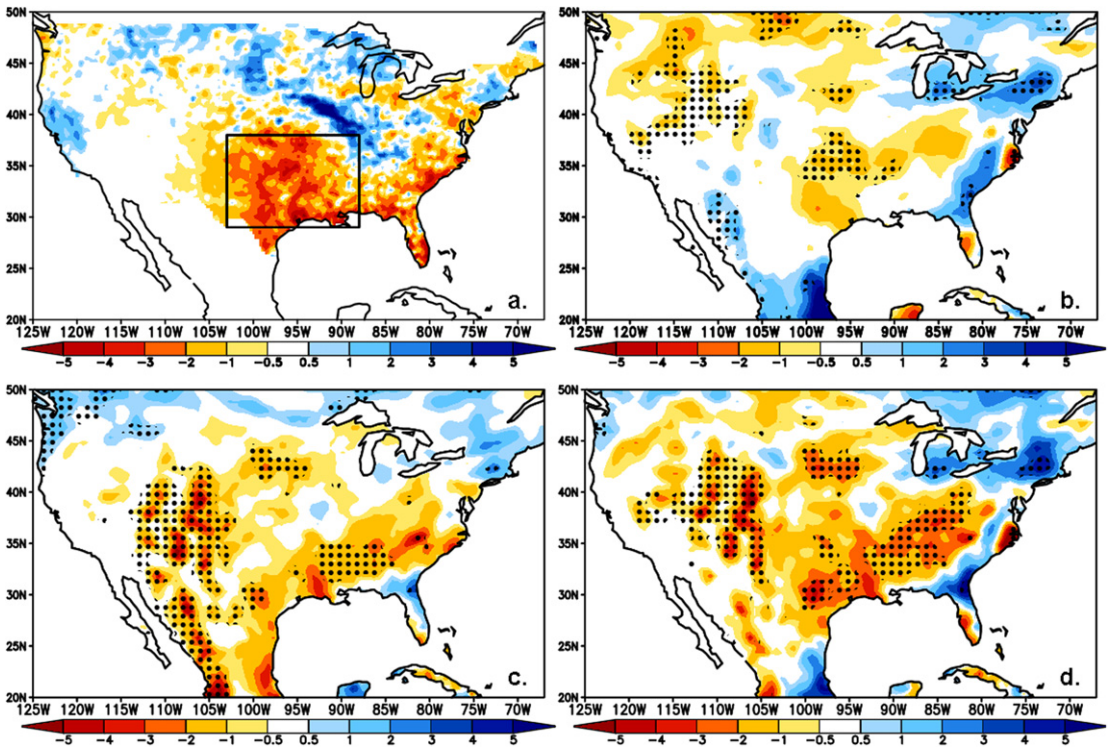

Figure 6. Observed/WRF simulated anomaly/difference of precipitation (mm/day) for June. (a) Observed, (b) SUBT effect, (c) SST effect, and (d) SST effect plus SUBT effect. The dotted areas denote statistical significance at the $\alpha = 0.01$ level of t-test values.

Table 2. Observed differences between years 2011 and the benchmarks and WRF-NMM simulated effects for different scenarios.

	Surface Temperature (K)			Precipitation (mm day-1)		
May	0.57	−0.06	−0.81	−0.99	−0.48	−0.04
June	3.45	1.18	2.40*	−2.31	−0.71**	−1.75**
July	3.15	1.22*	2.33**	−1.46	−1.05	−0.62

Averages over 88 °W–103 °W and 29 °N–38 °N.
*, **, and *** indicate statistics at 0.10, 0.05, and 0.02 significant levels, respectively.

and Case SUBTSST is expected to be closer to observed differences shown in figures 4(a), 5(a), and 6(a) if both SUBT and SST play roles in the drought. The observed anomaly and simulated June and July LST difference between Case 2011 and Case SUBT (referred to as SUBT effect), between Case 2011 and Case SST (referred to as SST effect), and between Case 2011 and Case SUBTSST (referred to as SUBT effect plus SST effect) are shown in Figures 4–5. The area averages of the differences over the SGP are summarized in table 2.

In summer 2011, the area of very warm temperatures was centered over Texas and Oklahoma, and included western portions of Louisiana and Arkansas, southern Kansas, and eastern New Mexico [3] (figures 4(a), 5(a)). Warm anomalies over the SGP in June are generally simulated with either SUBT effect or SST effect but the warm areas shift to the west with the SUBT effect (figures 4(b) and (c)). These two forcings seem to produce the warm anomalies over different areas. The LST anomaly in NWUS produced the statistically significant positive LST anomalies over west and southwest US (figure 4(b)). However, this anomaly is counteracted by negative LST anomalies caused by SST (figure 4(c)) such that only SST plus LST anomalies produce an adequate surface temperature anomaly pattern over SGP (figure 4(d)). At this point, we are unable to determine whether anomalies over west and southwest US are characteristics of NWUS LST anomaly effects or due to model deficiencies. Further modeling and case studies are needed to investigate this issue.

The SST effect (figure 4(c)) shows statistically significant impact over the southwest US and the Mexican Highlands. Heating over the Mexican Highlands coupled with the large-scale dynamical circulation can lead to heat advection over Texas and the southern Great Plains as reported in Myoung and Nielsen-Gammon [11]. Only SUBT effect plus SST effect combined produce better (statistically significant) spatial distribution of June heat anomalies over SGP (figure 4(d)) with comparable magnitude as observed (figure 4(a)). The spatial anomaly patterns in

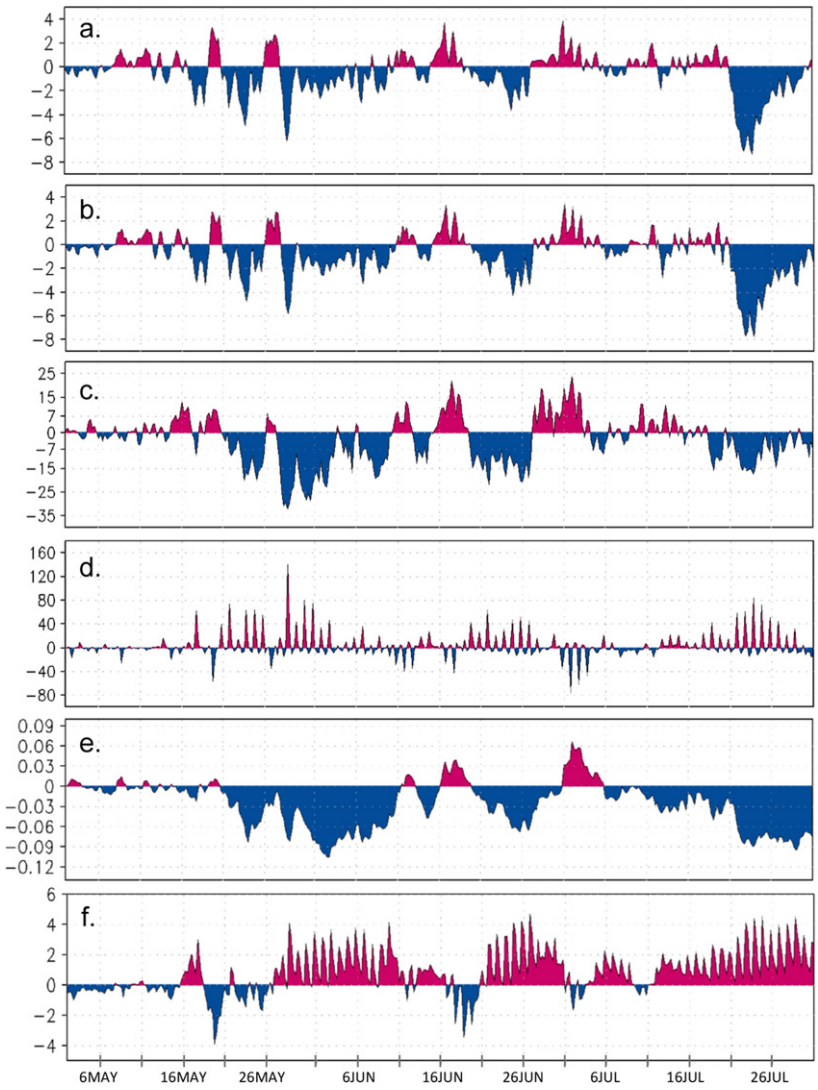

Figure 7. Time series of difference between Case 2011 and Case SUBT averaged over the SGP for (a) vertical integrated moisture flux divergence [mm day^{-1}], (b) precipitation [mm day^{-1}], (c) cloud cover [%], (d) net radiation [W m^{-2}], (e) soil wetness, and (f) surface temperature [°C].

figure 4(d) seem to be closer to those in figure 2(c) than the spatial patterns in 4(b) or 4(c) do. Table 2 shows that SUBT effect and SUBT effect plus SST effect produced about 34% and 70% of the observed June SGP heat anomaly, respectively. The observed July positive temperature anomaly extends to the north, with a slight southwest-northeast tilt of the anomaly area (figure 5(a)). Case SUBTSST (figure 5(d)) properly produces the spatial pattern of July hot anomaly over SGP because both SUBT and SST simulate better hot anomalies during this month than during June (figure 4). The SUBT effect produces about 40% of the hot anomaly, while the SUBT effect plus SST effect produces 74% of the anomaly.

The observed dry anomaly started to develop in May 2011 [37]. The SUBT effect properly simulated the dry summer conditions over the SGP (table 2). In June, observed dry anomaly conditions covered the southern US from Texas to Florida, with the drought centered over Texas (figure 6(a)). To the north, there was a slight positive rainfall anomaly over the Midwestern states. The SUBT effect properly produces the dry June conditions over the SGP but with smaller extent and lower intensity (figure 6(b)), showing about 31% of the actual rainfall anomaly (table 2). The combined effects of SUBT and SST produce both more accurate drought area and intensity (figure 6(d)), about 71% of the actual anomalies (table 2). Both cases also produce wet conditions to the north. In July, the extreme dry conditions relaxed (figure S3(a)). Although Case SUBT is still able to produce the drought conditions (table 2, figure S3(b)), it is not statistically significant. Case SST fails to produce drought, suggesting the difficulty in accurately simulating the dry area when the drought has weakened (figure S3), i.e., when the signal/noise ratio is small, it is difficult to properly simulate the anomaly with statistical significance.

To delineate how the hot and dry conditions developed over the SGP, figure 7 shows the daily time series

of differences for several variables between Case 2011 and Case SUBT averaged over the SGP—i.e., the SUBT effect. The cold temperature anomaly in the NWUS produces an anomalous planetary wave pattern across North America (figure S4). The negative vorticity anomaly (10^6 s^{-1}) at 500 hPa along the west coastal area averaged over 35 °N and 50 °N due to the SUBT propagates to the east (figure S5). Similar processes—but with opposite anomalies—have been comprehensively discussed in [34]. The vertically integrated moisture flux divergence (MFD) associated with negative vorticity over the SGP starts in the second half of May (figure 7(a)). Strong MFD persists in June and July, associated with an anticyclonic circulation pattern (positive geopotential anomaly) in the central US, and low precipitation (figure 7(b)). Geopotential highs have been associated with previous heatwave cases in the Midwest [46] and the European heatwave of 2003 [47], tending to block the zonal circulation and producing stationary wave warm advection. Figures 7(a) and (b) also show that the MFD almost equals the precipitation reduction during late May. As progressing into June and July, however, the contribution of MFD to precipitation reduction is reduced from 96% in May to about 65% in June and July. Negative soil moisture anomalies (figure 7(e)) and corresponding low evaporation start to develop in response to the low precipitation. Studies have shown that a lack of rainfall in the main rainfall season extending from April–June can set up a dry soil-induced temperature positive feedback over this region. By July local land surface temperature feedbacks tend to dominate over large-scale circulation across the SGP [48].

During the same three-month time period, cloud cover is reduced accordingly (figure 7(c)), leading to more short wave radiation reaching the ground and contributing to positive net radiation (figure 7(d)), which combined with low evapotranspiration contribute to a high downward ground heat flux, leading to high surface temperature (figure 7(f)).

4. Discussion and conclusions

While numerous studies have focused on the teleconnection between SST anomalies and US drought, the remote effect of large-scale land temperature anomalies on regional droughts has been largely ignored. Our previous case study [34] established the theoretical base for this teleconnection. The observational evidence and modeling study presented here suggest that the associated strength in observations between antecedent early May SUBT anomaly in the NWUS and summer precipitation anomalies over the SGP is likely larger than random internal atmospheric variations arising from the chaotic variability of the atmosphere; table 1 has shown that the observed correlation coefficients for SST and for NWUS LST are comparable. Our model study shows that the SST effect produces 45% and LST produces 31% of the observed rainfall anomaly, respectively. The latter is smaller than SST effects, but it is still a first order effect. Specifically, it is shown that cold spring NWUS land temperature anomalies are a factor in increasing the probability of dry and hot conditions in the SGP, while atmospheric internal variability and other factors also contribute substantially to year-to-year variance. More case studies are needed to fully understand the role of LST effect.

Furthermore, since the May SST anomalies during the years with cold NWUS LST anomalies are rather weaker compared with the LST anomalies (figure 2(a)), and since LST and SST effects show different geographical characteristics [figures 4(b) and (c), 5(b) and (c), 6(b) and (c), S2(b) and (c)], the relationship between LST and SST and other variables needs to be further investigated. It should also be pointed out that despite the imposed large initial LST and SUBT anomaly [figure 3(a)], the simulated May LST surface temperature difference between Case 2011 and Case SUBT is still weaker than the observational benchmark (figure S6(b)), which imply that this model simulated LST effect could be underestimated. Since the relationship between May SST in NEP and LST is not that strong (figures 2(a) and S6(c)), the cause of the deficiency in holding the May LST anomaly in simulations due to other causes, such as the shortcoming in land surface model or failure in producing proper snow memory effect, etc, needs to be further investigated.

In this study, we find that although GCM simulations produced the SGP June drought and large anomalous heat, the drought spatial patterns were not very consistent with the observations, and the July hot conditions were not reproduced (table S1). We therefore focused on the use and analysis of RCM simulations in this study. The improvement of regional climate simulations using RCM downscaling has been reviewed in other papers [49, 50].

To more comprehensively understand the role of antecedent spring land surface temperature anomaly in the NWUS on the remote summer drought in the Great Plains, more case studies with different models and external forcings from different SST, SUBT, and soil moisture sources are necessary. To further evaluate the strength of this relationship and associated mechanisms, other high profile North American extreme events such as the North Great Plain drought since 2012 (listed in the NOAA MAPP Drought Task Force [51]) and the 2015 Texas Flood should be used as additional case studies in future work.

Climate change and variability cause extreme regional responses at different spatial and temporal scales. Over the past 30 years, both winter and spring in the NWUS have seen an increase in average precipitation [52]. The NWUS spring LST anomalies are significantly negatively correlated to the antecedent snow extent and precipitation (cf section 3.1), which seems to be consistent with the intensified

precipitation decrease in Central US since 1979 [17]. The analysis based on the Coupled Model Intercomparison Project Phase 5 (CMIP5) simulations suggests there will be more winter precipitation in the northwest US with high agreement [53]. According to our and others' analyses, this would cause a cold winter and spring. Another study also based on CMIP5 suggests unprecedented 21st century drought risk in the Central Plains [54]. All these results seem to support our hypothesis that cold spring in NWUS has a potentially high possibility of causing a dry summer in SGP. The results of our study suggest the potential for more skillful seasonal predictions of US droughts, particularly in the Great Plains.

Acknowledgement

This work was supported by National Science Foundation grants AGS-1346813, AGS-1115506, and AGS-1540518. We thank Mr John Mioduszewski and Mr Thomas Estilow of Rutgers University for the snow data. The authors also thank Professor Jared Diamond and Professor David Rigby of UCLA for their comments and contributions to the manuscript revisions, as well as two anonymous reviewers' very constructive comments/suggestions to help improve the paper. The model runs were conducted at the National Center for Atmospheric Research Bluefire Supercomputer and the Texas Advanced Computer Center Stampede Supercomputer.

References

[1] Andreadis K M, Clark E A, Wood A W, Hamlet A F and Lettenmaier D P 2005 Twentieth-century drought in the conterminous United States *J. Hydromet.* **6** 985–1001
[2] Barlow M, Nigam S and Berbery E H 2001 ENSO, pacific decadal variability, and US summer time precipitation, drought, and stream flow *J. Clim.* **14** 2105–28
[3] Hoerling M, Kumar A, Dole R, Nielsen-Gammon J W, Eischeid J, Perlwitz J, Quan X, Zhang T, Pegion P and Chen M 2013 Anatomy of an extreme event *J. Clim.* **26** 2811–32
[4] Groisman P Y and Knight R W 2008 Prolonged dry episodes over the conterminous United States: new tendencies emerging during the last 40 years *J. Clim.* **21** 1850–62
[5] Woodhouse C A and Overpeck J T 1998 2000 years of drought variability in the central United States *Bull. Am. Meteorol. Soc.* **79** 2693–714
[6] Hoerling M *et al* 2014 Causes and predictability of the 2012 Great Plains drought *Bull. Am. Meteorol. Soc.* **95** 269–82
[7] Karl T R and Quayle R G 1981 The 1980 summer heat wave and drought in historical perspective *Mon. Weather Rev.* **109** 2055–73
[8] Hong S-Y and Kalnay E 2002 The 1998 Oklahoma–Texas drought: mechanistic experiments with NCEP global and regional models *J. Clim.* **15** 945–63
[9] Oglesby R J and Erickson D J III 1989 Soil moisture and the persistence of North American drought *J. Clim.* **2** 1362–80
[10] Zhu C M, Leung L R, Gochis D, Qian Y and Lettenmaier D P 2009 Evaluating the influence of antecedent soil moisture on variability of the North American Monsoon precipitation in the coupled MM5/VIC modeling system *J. Adv. Model. Earth Syst.* **1** 13
[11] Myoung B and Nielsen-Gammon J W 2010 The convective instability pathway to warm season drought in Texas: I. The role of convective inhibition and its modulation by soil moisture *J. Clim.* **23** 4461–73
[12] Xue Y, Fennessy M J and Sellers P J 1996 Impact of vegetation properties on US summer weather prediction *J. Geophys. Res.* **101** 7419–30
[13] Trenberth K E, Branstator G W and Arkin P A 1988 Origins of the 1988 North American drought *Science* **242** 1640–5
[14] Ting M and Wang H 1997 Summertime US precipitation variability and its relation to Pacific sea surface temperature *J. Clim.* **10** 1853–73
[15] Nigam S, Guan B and Ruiz-Barradas A 2011 Key role of the Atlantic multidecadal oscillation in 20th century drought and wet periods over the Great Plains *Geophys. Res. Lett.* **38** L16713
[16] Schubert S *et al* 2009 A US CLIVAR project to assess and compare the responses of global climate models to drought-related SST forcing patterns: overview and results *J. Clim.* **22** 5251–72
[17] Wang S Y S *et al* 2015 An intensified seasonal transition in the Central US that enhances summer drought *J. Geophys. Res. Atmos.* **120** 8804–16
[18] Rajagopalan B, Cook E, Lall U and Ray B K 2000 Spatiotemporal variability of ENSO and SST teleconnections to summer drought over the United States during the twentieth century *J. Clim.* **13** 4244–55
[19] Mo K C, Schemm J-K E and Yoo S-H 2009 Influence of ENSO and the Atlantic multidecadal oscillation on drought over the United States *J. Clim.* **22** 5962–82
[20] Rui R and Wang G 2011 Impact of sea surface temperature and soil moisture on summer precipitation in the United States based on observational data *J. Hydromet.* **12** 1086–99
[21] Seager R *et al* 2014 Dynamical causes of the 2010/11 Texas–northern Mexico drought *J. Hydromet.* **15** 39–68
[22] Chen M, Xie P, Janowiak J E and Arkin P A 2002 Global land precipitation: a 50-yr monthly analysis based on gauge observations *J. Hydromet.* **3** 249–66
[23] Ropelewski C F, Jonowiak J E and Halper M E 1985 The analysis and display of real time surface climate data *Mon. Weather Rev.* **113** 1101–7
[24] Xue Y, Sellers P J, Kinter J L III and Shukla J 1991 A simplified biosphere model for global climate studies *J. Clim.* **4** 345–64
[25] Dickinson R E 1988 The force-restore model for surface temperature and its generalization *J. of Clim.* **1** 1086–97
[26] Higgins R W and Shi W 2000 Dominant factors responsible for interannual variability of the summer monsoon in the southwestern United States *J. Clim.* **13** 759–76
[27] Gutzler D S 2000 Covariability of spring snowpack and summer rainfall across the southwest United States *J. Clim.* **13** 4018–27
[28] Hu Q and Feng S 2004 A Role of the soil enthalpy in land memory *J. Clim.* **17** 3633–43
[29] Robock A, Mu M, Vinnikov K and Robinson D 2003 Land surface conditions over Eurasia and Indian summer monsoon rainfall *J. Geophys. Res.* **108** 4131
[30] Barnett T P, Pierce D W, Latif M, Dommenget D and Saravanan R 1999 Interdecadal interactions between the tropics and midlatitudes in the Pacific basin *Geophys. Res. Lett.* **26** 615–8
[31] Leathers D J and Robinson D A 1983 The association between extremes in North American snow cover and United States temperature *J. Clim.* **6** 1345–55
[32] Cayan D R 1966 Interannual climate variability and snowpack in the western United States *J. Clim.* **9** 928–48
[33] Guo W, Sun S and Qian Y 2002 Case analyses and Numerical Simulation of soil thermal impacts on land surface energy budget based on an off-line land surface model *Adv. Atmos. Sci.* **19** 500–12
[34] Xue Y, Vasic R, Janjic Z, Liu Y M and Chu P C 2012 The impact of spring subsurface soil temperature anomaly in the western US on North American summer precipitation—a case study using regional climate model downscaling *J. Geophys. Res.* **117** D11103

[35] Peterson T C, Stott P A and Herring S 2012 Explaining extreme events of 2011 from a climate perspective *Bull. Am. Meteorol. Soc.* **93** 1041–67
[36] Tadesse T, Wardlow B D, Brown J F, Svoboda M D, Hayes M J, Fuchs B and Gutzmer D 2015 Assessing the vegetation condition impacts of the 2011 drought across the US Southern Great Plains using the vegetation drought response index (VegDRI) *J. Appl. Meteo. and Clim.* **54** 153–69
[37] Blunden J and Derek A S 2012 State of the climate in 2011 *Bull. Am. Meteorol. Soc.* **93** 1–282
[38] Luo L and Zhang Y 2012 Did we see the 2011 summer heat wave coming? *Geophys. Res. Lett.* **39** L09708
[39] Rupp D E, Li S, Massey N, Sparrow S N, Mote P W and Allen M 2015 Anthropogenic influence on the changing likelihood of an exceptionally warm summer in Texas, 2011 *Geophys. Res. Lett.* **42** 2392–400
[40] Robinson D A 2012 Snow blitz, the US 2010–2011 snow report *Weatherwise* March/April **65** 28–37 (www.weatherwise.org)
[41] Kanamitsu M, Alpert J C, Campana K A, Caplan P M, Deaven D G, Iredell M, Katz B, Pan H-L, Sela J and White G H 1991 Recent changes implemented into the global forecast system at NMC *Wea. and Forecasting* **6** 425–35
[42] Janjic Z *et al* 2014 User's Guide for the NMM Core of the Weather Research and Forecast (WRF) Modeling System Version 3 (http://dtcenter.org/wrf-nmm/users/) Developmental Testbed Center/National Centers for Environmental Prediction, Bounlder p 213
[43] Kanamitsu M, Ebisuzaki W, Woollen J, Yang S-K, Hnilo J J, Fiorino M and Potter G L 2002 NCEP–DOE AMIP-II reanalysis (R-2) *Bull. Amer. Meteor. Soc.* **83** 1631–43
[44] Shukla J and Mintz Y 1982 Influence of land-surface evapotranspiration on the Earth's climate *Science* **19** 1498–501
[45] Dickinson R E and Henderson-Sellers A A 1988 Modeling tropical deforestation: a study of GCM land-surface parameterizations *Q. J. R. Meteorol. Soc.* **114** 439–62
[46] Kunkel K E, Changnon S S, Reike B and Arritt R W 1996 The July 1995 heat wave in the Midwest: a climatic perspective and critical weather factors *Bull. Amer. Meteor. Soc.* **77** 1507–18
[47] Fischer E M, Seneviratne S I, Vidale P L, Luthi D and Schar C 2007 Soil moisture—atmosphere interactions during the 2003 European summer heat wave *J. Clim.* **20** 5081–99
[48] Trenberth K E and Shea D J 2005 Relationships between precipitation and surface temperature *Geophys. Res. Lett.* **32** L14703
[49] Xue Y, Jajnic Z, Dudhia J, Vasic R and De Sales F 2014 A review on regional dynamical downscaling in intra-seasonal to seasonal simulation/prediction and major factors that affect downscaling ability *Atmos. Res.* **147-148** 68–85
[50] Leung L R, Mearns L O, Giorgi F and Wilby R L 2003 Regional climate research: needs and opportunities *Bull. Am. Meteorol. Soc.* **84** 89–95
[51] Mariotti A, Schubert S, Mo K, Peters-Lidard C, Wood A, Pulwarty R, Huang J and Barrie D 2013 Advancing drought understanding, monitoring, and prediction *Bull. Amer. Meteor. Soc.* **94** ES186–8
[52] Higgins R W and Kousky V E 2013 Changes in observed daily precipitation over the United States between 1950–79 and 1980–2009 *J. Hydromet.* **14** 105–21
[53] Neelin J D, Langenbrunner B, Meyerson J E, Hall A and Berg N 2013 California winter precipitation changes under global warming in the coupled model intercomparison project phase 5 ensemble *J. Clim.* **26** 6238–56
[54] Cook B I, Ault T R and Smerdon J E 2015 Unprecedented 21st century drought risk in the American Southwest and Central Plains *Science Advances* **1** e1400082

Corrigendum: Spring land temperature anomalies in northwestern US and the summer drought over Southern Plains and adjacent areas (2016 *Environ. Res. Lett*. **11** 044018)

2016 Environ. Res. Lett. 11 059502

(http://iopscience.iop.org/1748-9326/11/5/059502)

Environmental Research Letters

CORRIGENDUM

Corrigendum: Spring land temperature anomalies in northwestern US and the summer drought over Southern Plains and adjacent areas (2016 *Environ. Res. Lett.* **11** 044018)

OPEN ACCESS

PUBLISHED
20 May 2016

Yongkang Xue[1,2], **Catalina M Oaida**[2], **Ismaila Diallo**[1], **J David Neelin**[2], **Suosuo Li**[1,3], **Fernando De Sales**[1,4], **Yu Gu**[2], **David A Robinson**[5], **Ratko Vasic**[6] **and Lan Yi**[7]

[1] Department of Geography, University of California, Los Angeles, CA 90095, USA
[2] Department of Atmospheric & Oceanic Sciences, University of California, Los Angeles, CA 90095, USA
[3] Cold and Arid Regions Environmental and Engineering Research Institute, Chinese Academy of Sciences, Lanzhou, 730000, People's Republic of China
[4] San Diego State University, San Diego, CA 92182, USA
[5] Department of Geography, Rutgers University, Piscataway, NJ 08854, USA
[6] National Center for Environmental Prediction, College Park, MD 20740, USA
[7] Chinese Academy of Meteorological sciences, Beijing, 10081, People's Republic of China

E-mail: yxue@geog.ucla.edu

Table 2 in the original version of this paper accidently omits row two, which explains what the various statistics represent (i.e. observations, SUBT effect, SUBT + SST effects). The complete version of table 2 should read as below. The statistics in this table have not changed. The table simply includes additional headers for clarity. This correction to table 2 does not affect understanding the results, discussion, or conclusions found in the original manuscript.

Table 2. Observed differences between year 2011 and the benchmark as well as differences between various WRF-NMM simulated cases, highlighting the SUBT and SUBT+SST effects.

	Surface temperature (K)			Precipitation (mm d^{-1})		
	Observation	SUBT effect	SUBT + SST effects	Observation	SUBT effect	SUBT + SST effects
May	0.57	−0.06	−0.81	−0.99	−0.48	−0.04
June	3.45	1.18	2.40*	−2.31	−0.71**	−1.75**
July	3.15	1.22*	2.33**	−1.46	−1.05	−0.62

Average area: 88 W–103 W and 29 N–38 N.
*, **, and ***: statistics at 0.10, 0.05, and 0.02 significant levels, respectively.

Figure S1: Observed May SST difference (ºC) between 9 coldest years and the 9 warmest years based on SST Anomalies. The dotted areas denote the statistical significance at the α=0.01 level of t-test values.

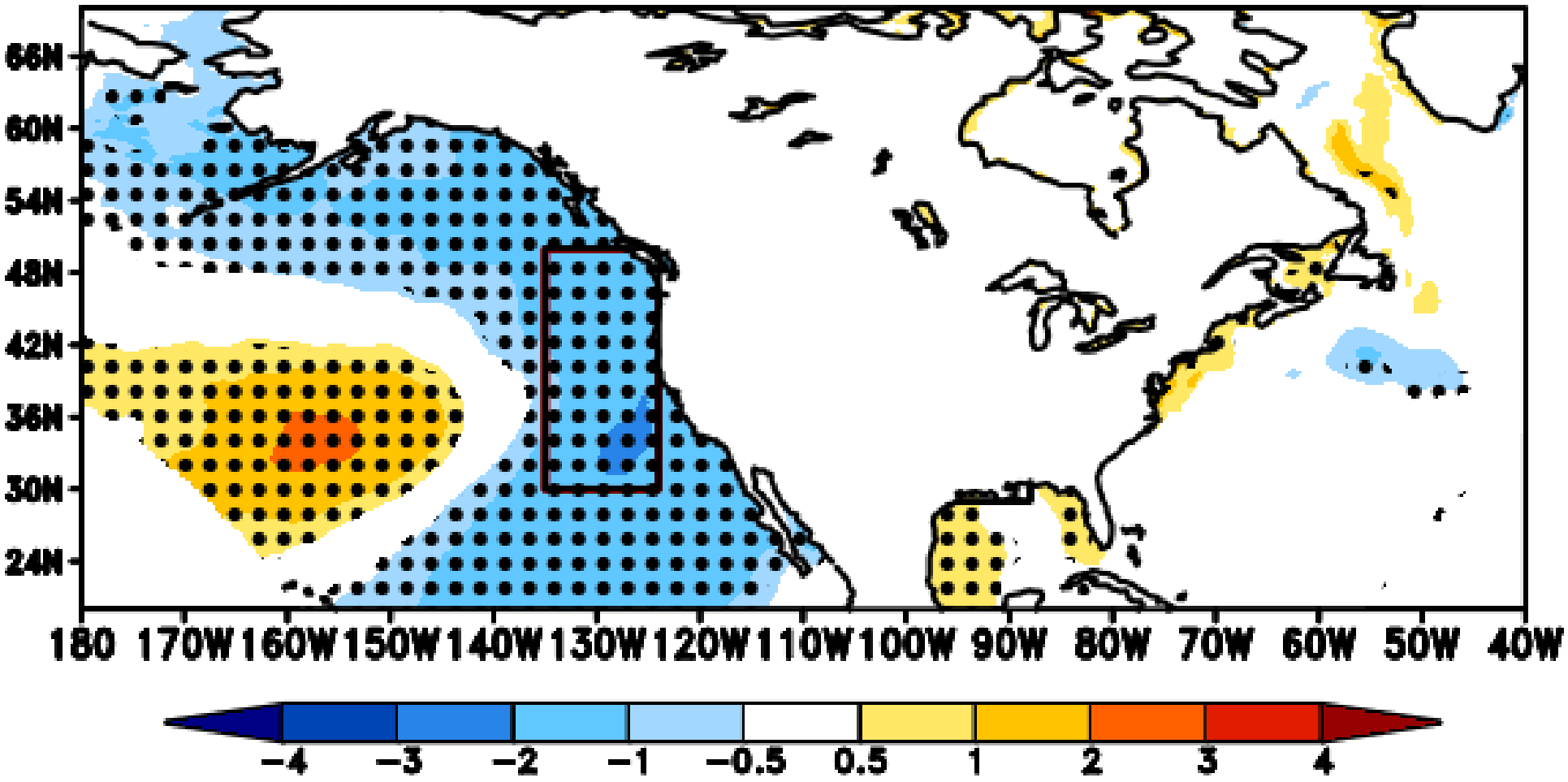

Figure S2. Mean surface temperature (ºC) and precipitation (mm day^{-1}) for June 2011 from CAMs and GTS observations and WRF-NMM simulation.

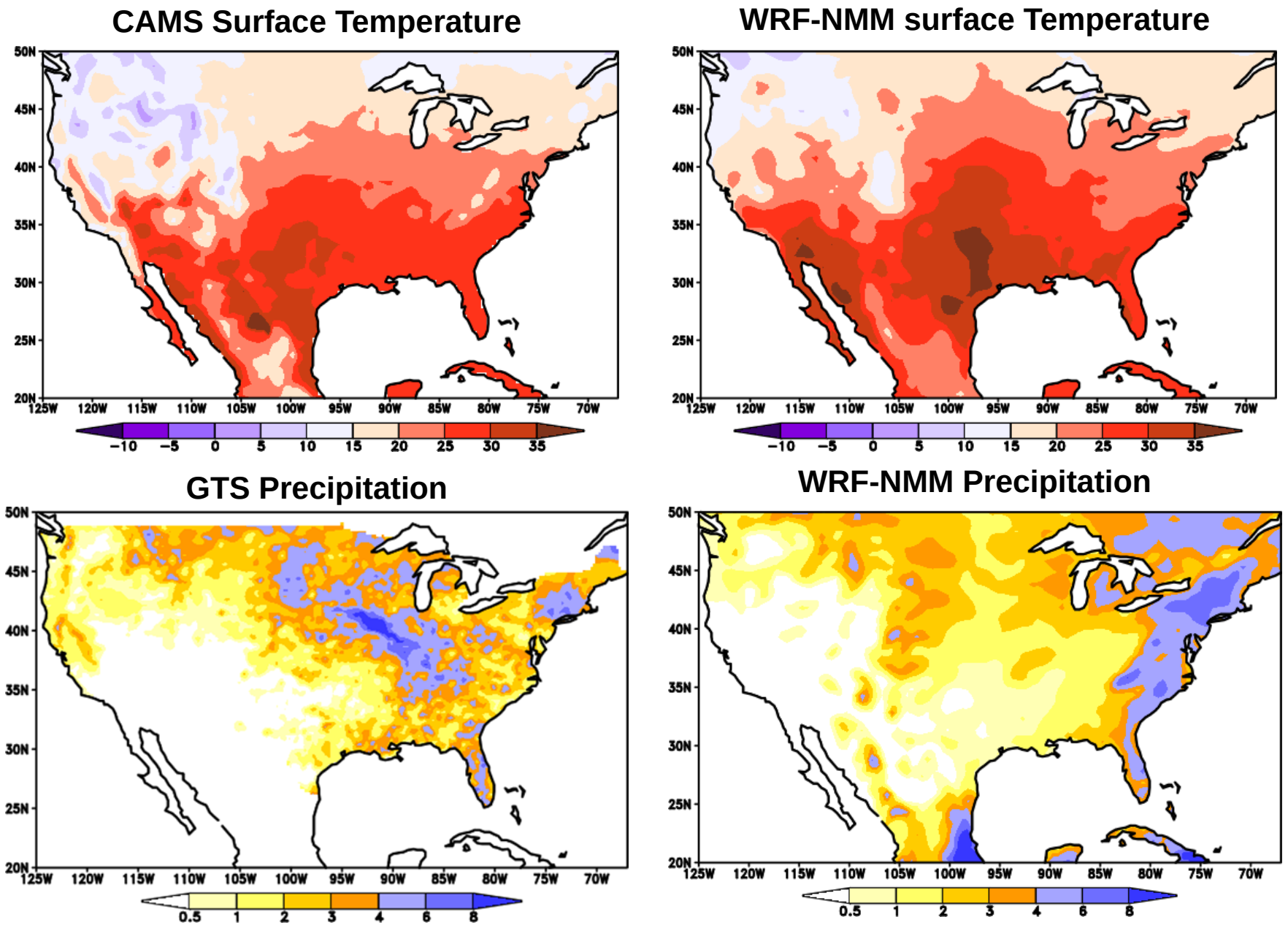

Figure S3. Observed/WRF simulated anomaly/difference of precipitation (mm/day) for July. (a) Observed; (b) SUBT effect; (c) SST Effect; (d) SST effect plus SUBT effect. The dotted areas denote statistical significance at the α=0.01 level of t-test values.

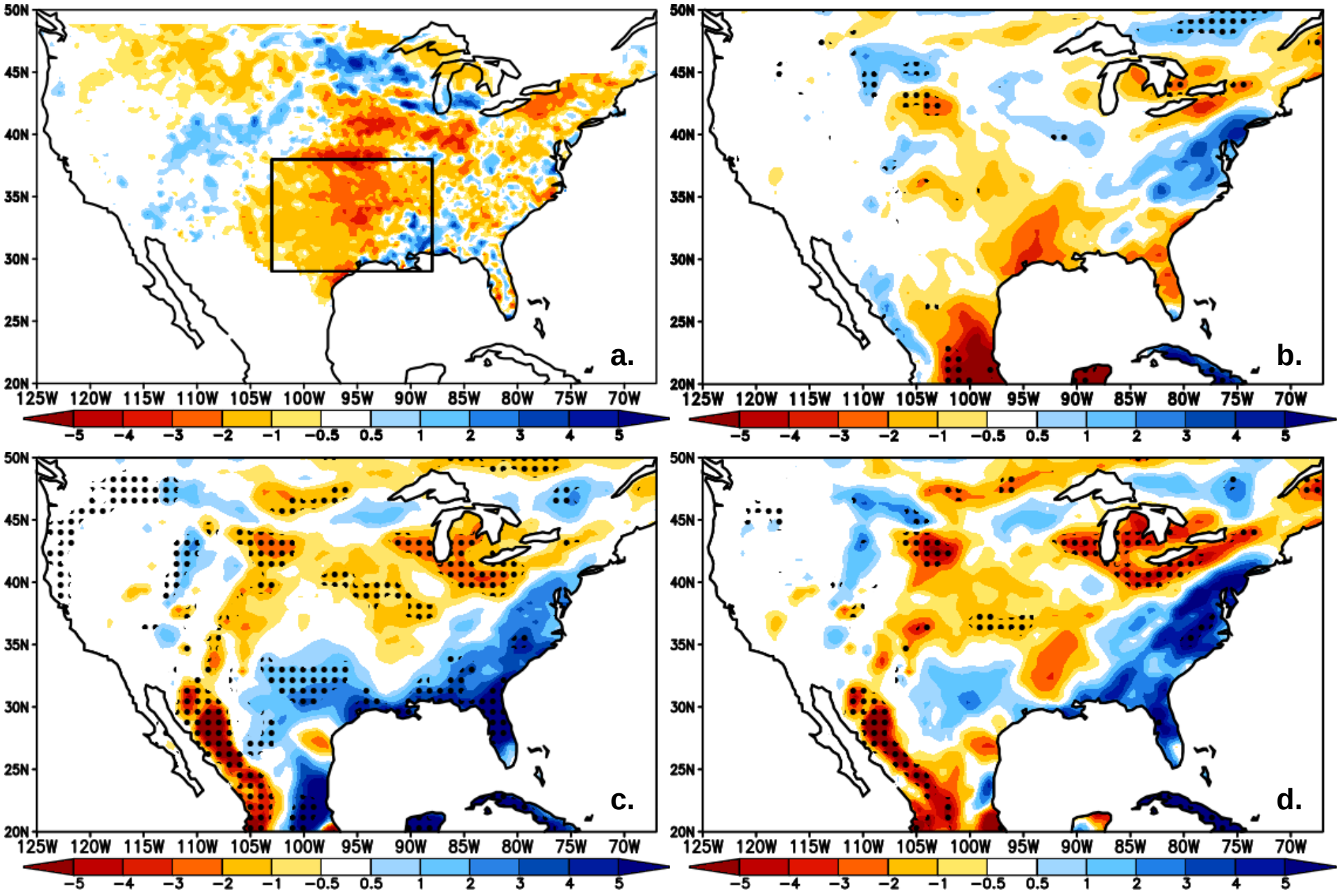

Figure S4. Simulated 16-31 May geopotential height (GPM) difference at 500 hPa between Case 2011 and Case SUBT.

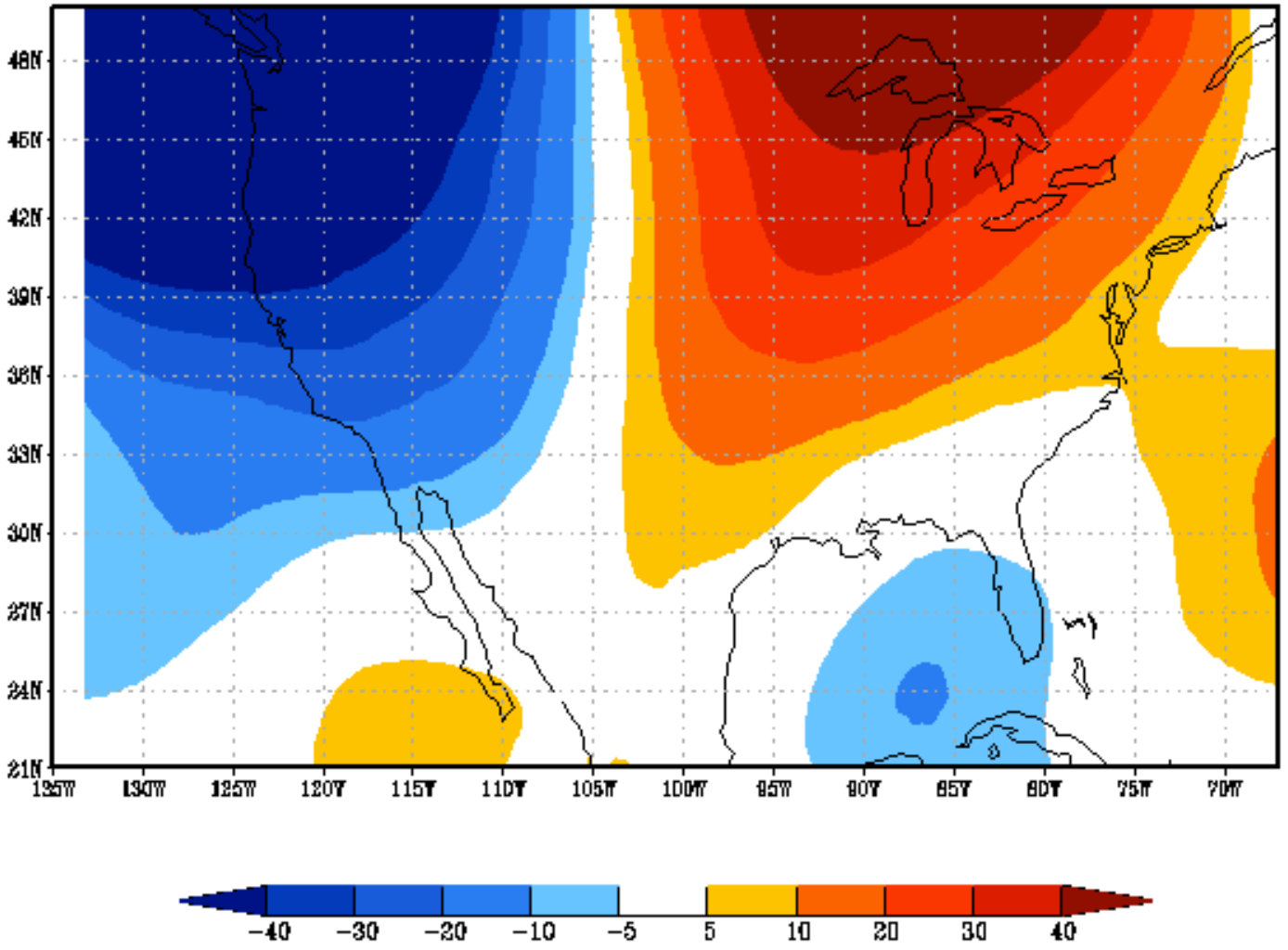

Figure S5. Perturbation pathway: temporal-zonal cross section of vorticity anomaly (10^6 s^{-1}) at 500 hPa averaged over 35N and 50N.

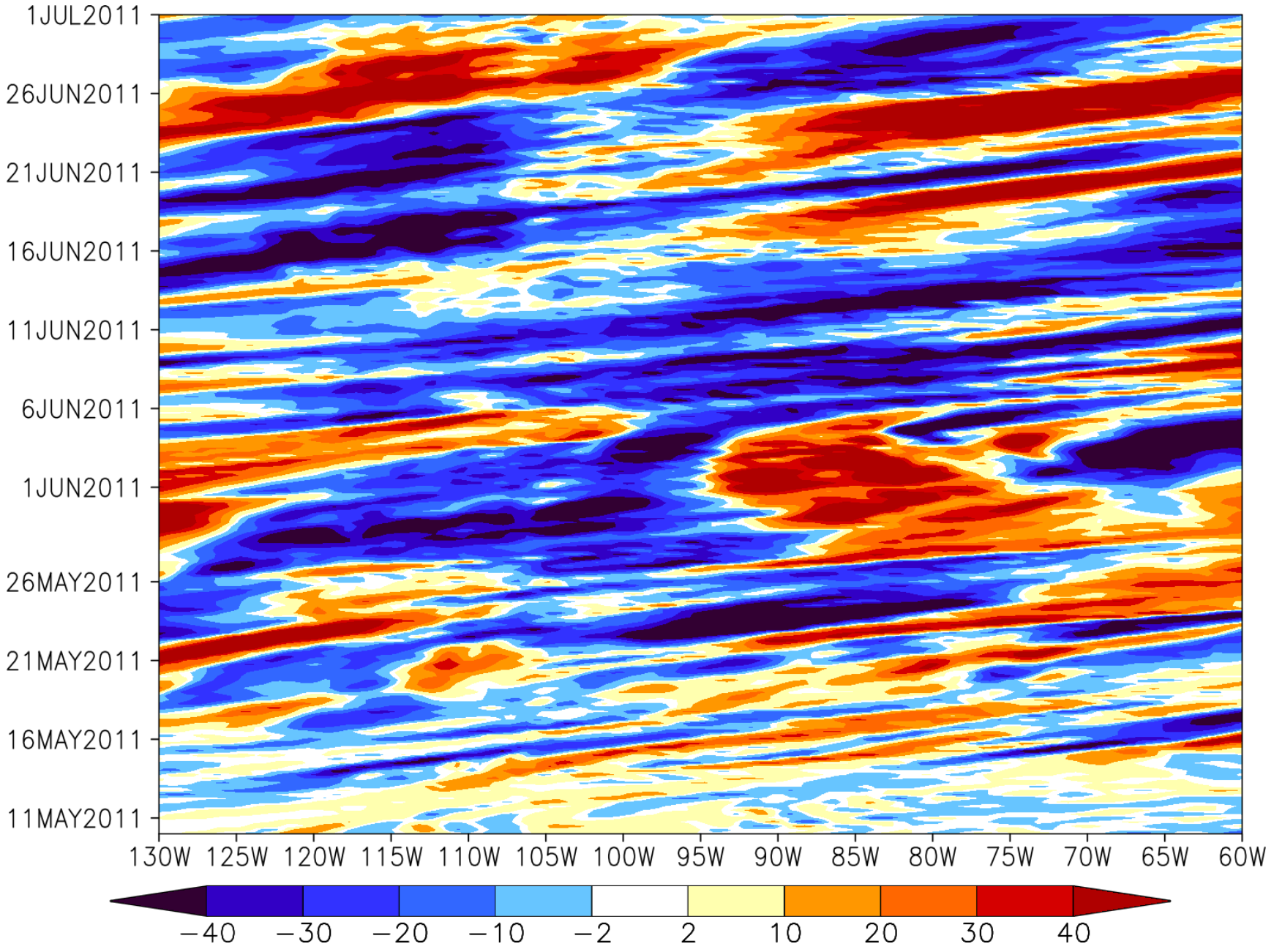

Figure S6. Observed/WRF simulated anomaly/difference of surface temperature (ºC) for May. (**a**) Observed; (**b**) SUBT effect; (**c**) SST Effect. The dotted areas denote statistical significance at the α=0.01 level of t-test values.

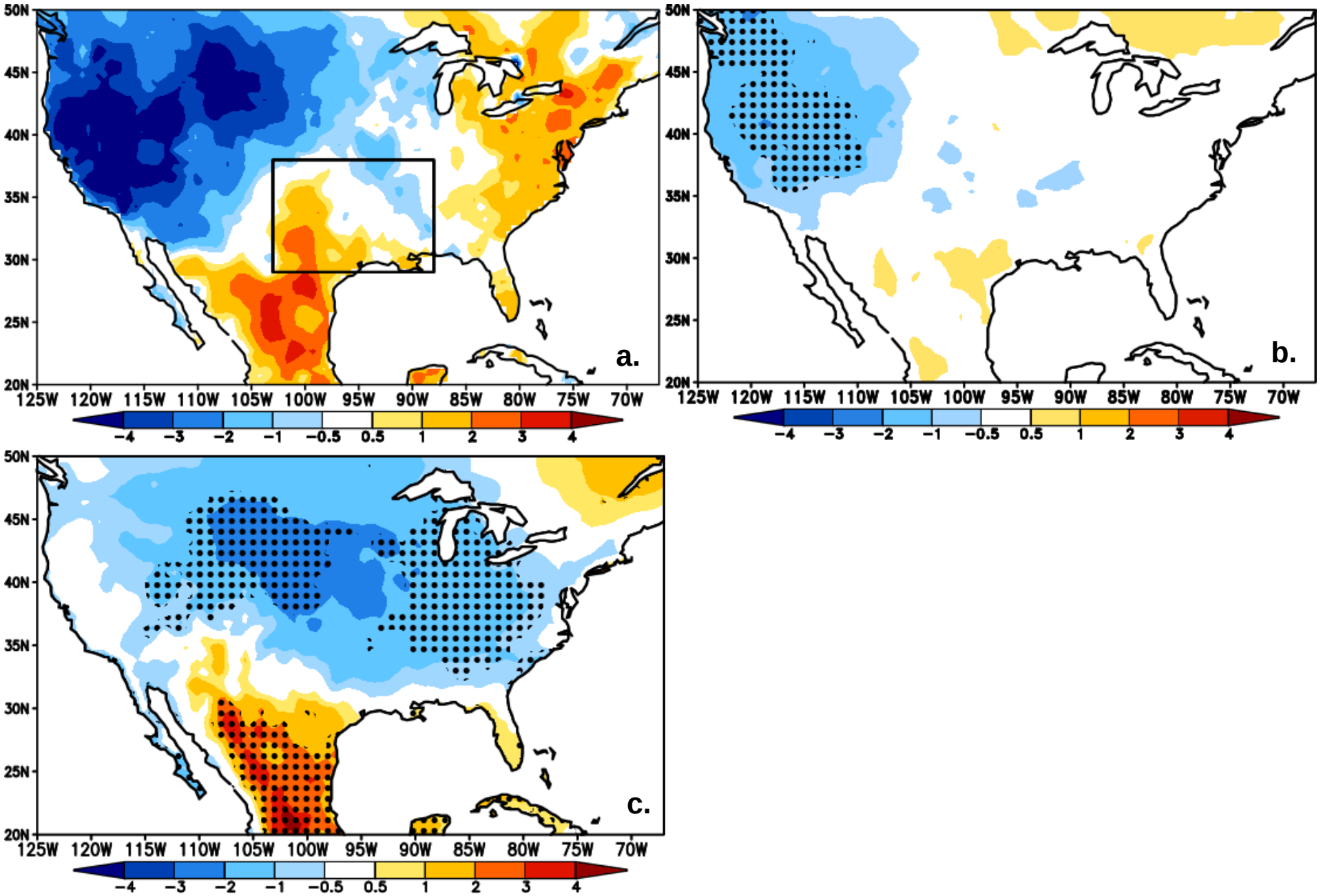

Table S1. Observed differences between year 2011 and the benchmarks, and GCM-simulated differences for different scenarios

	Surface Temperature (K)			Precipitation (mm day^{-1})		
	Observation	SUBT effect	SUBT+SST	Observation	SUBT effect	SUBT+SST
May	0.57	0.04	0.11	-0.99	-0.04	-0.24
June	3.45	1.43	2.87**	-2.31	-0.86*	-2.44***
July	3.14	0.10	1.62	-1.46	-0.67	-0.95

Note: 1). Average area: 88W – 103W and 29N – 38N.

2). *,**, and *** indicates statistically significance at 0.05, 0.02, and 0.001 levels, respectively.